[56]S. Bjørnholm and J. E. Lynn, unpublished preliminary results.
[57]P. Möller, Nucl. Phys. (to be published).
[58]B. B. Back, H. C. Britt, J. D. Garrett, and O. Hansen, Phys. Rev. Letters 28, 1707 (1972).
[59]U. Mosel, Phys. Rev. C 6, 971 (1972).
[60]R. Vandenbosch, Phys. Rev. C 5, 1428 (1972).
[61]P. A. Seeger, in Proceedings of the Fourth International Conference on Atomic Masses and Fundamental Constants, Teddington, England, 1971 (to be published).

PHYSICAL REVIEW C VOLUME 7, NUMBER 2 FEBRUARY 1973

Neutron Resonance Spectroscopy. XI. The Separated Isotopes of Yb†

H. I. Liou, H. S. Camarda,* G. Hacken, F. Rahn, J. Rainwater, M. Slagowitz, and S. Wynchank‡
Columbia University, New York, New York 10027
(Received 26 July 1972)

Neutron time-of-flight resonance spectroscopy results, using the Nevis synchrocyclotron, for the separated Yb isotopes (170, 171, 172, 173, 174, 176) are given. Transmission and self-indication measurements were made for several sample thicknesses of each isotope. Resonance parameters, Γ_n^0 (or $g\Gamma_n^0$), are given to ~1.8 keV for 171 and 173, and to ~10 keV for 172, 174, and 176. Levels in 170 were those seen in the natural element, but not in the 171–176 isotopes. Many resonance Γ_γ and J values were also obtained for 171 and 173, and a few Γ_γ values for 172 and 174. The $10^4 S_0$ values are 2.25± 1.0, 1.86± 0.16, 1.68± 0.20, 1.60 ± 0.28, 1.62± 0.21, and 2.29± 0.32 for 170, 171, 172, 173, 174, and 176, respectively. $\langle\Gamma_\gamma\rangle$ = 76.5 meV (37 levels), 72.3 meV (3 levels), and 73.8 meV (33 levels) for 171, 172, and 173, respectively. A shape fit to the asymmetric level in 174 at 342.7 eV gave $R' = (7.9 \pm 0.5)$ fm. The increasing σ below ~100 eV for 174 and natural Yb, and the known thermal 174 partial cross sections, were fitted assuming a bound 174 level at $E_0 = -25$ eV, $\Gamma_n^0 = 160$ meV. Comparison of the $(g\Gamma_n^0)^{1/2}$ distributions with Porter-Thomas theory and the nearest-neighbor energy spacings with the Wigner theory gave best agreement for 172, as did other statistical orthogonal ensemble (O.E.) tests. There were missing weak s levels for 171 and 173 and extra p levels for 176. The 174 and 176 results were also compatible with O.E. theory but provided poorer test cases than 172.

I. INTRODUCTION

This is the eleventh in a series of papers[1] reporting results of high-resolution neutron resonance time-of-flight spectroscopy using the Columbia University Nevis synchrocyclotron as a source. The paper presents resonance parameter results for the separated isotopes of Yb over the energy range to 1.7 or 1.8 keV for the odd isotopes ^{171}Yb and ^{173}Yb, and to 10 or 20 keV for the even isotopes ^{172}Yb, ^{174}Yb, and ^{176}Yb. In addition, we have measurements using natural Yb samples which permit us to evaluate level parameters for a number of levels of ^{170}Yb (3.03 at.% in natural Yb) to ~1300 eV which are not hidden by levels in the more abundant isotopes. Our study of the Yb isotopes has extended over a number of years. The analysis of earlier Yb data obtained was given in the Columbia University Ph.D. thesis of Liou. Since the measurements obtained later were of such superior quality to our earlier measurements, publication was delayed to permit a thorough analysis of the data which form the main basis for this paper. Liou has been mainly responsible for this data analysis, while all of the authors were involved in carrying through the later measurements.

We have previously reported results (VIII) for some of the other data obtained during these measurements, along with a description of the experimental details and data analysis techniques. The Er results, especially for ^{166}Er, gave the first conclusive evidence supporting the statistical orthogonal ensemble (O.E.) theory for the systematics of level spacings for single s populations. This was supported by the results (IX) for ^{152}Sm and some other favorable nuclei[2] in the mass range $150 \leq A \leq 190$. The agreement with the theory is also excellent for ^{172}Yb which is discussed in this paper. The most favorable nuclei for such tests (in this mass interval) seem to be the lowest-mass even-even isotopes having relatively high abundance in the natural elements. It is a mass region where there is a peak in the s strength function, S_0, and the p strength function S_1 is appreciably smaller. The effect favoring the lightest even-even isotope for a given element presumably relates to a trend for S_0 to decrease as neutrons are added for a given Z, coupled with a corresponding increase in S_1. These effects have been mentioned by others.[3] While this trend for Yb seems to be generally fol-

lowed, the value of S_0 for ^{176}Yb seems to increase again relative to ^{174}Yb. An additional consideration relates to the rapid increase in average level spacing for even-even isotopes as the neutron number increases, since the binding of the extra neutron decreases. The binding energies for an extra neutron added to Yb, $A=170$, 171, 172, 173, 174, and 176 are, respectively, 6.760, 8.140, 6.480, 7.440, 5.840, and 5.530 MeV.

In addition to previous published results for the Yb isotopes reviewed to 1966[4] in BNL-325, there has been an important paper by Mughabghab and Chrien[5] presenting results using a fast chopper at the Brookhaven reactor. Their measurements involve considerably poorer energy resolution than ours, but they use only ~12×38-mm transmission sample area (vs our 32×127-mm area) so they can use "thicker samples" for isotopes where only very small sample masses are available. Since their facility is continuously available, they can accumulate good statistical accuracy by using longer counting intervals (than we do). An example of this occurs for the low natural abundant ^{170}Yb sample for which only very small sample size of the separated isotope is available, but for which they have resonance results to 450 eV. Most of the extra resonances which we observe in natural Yb, but not in the 171, 172, 173, 174, or 176 isotope samples are due to ^{170}Yb, and we agree with their assignments where our energy ranges overlap.

II. EXPERIMENTAL DETAILS

The description of the experimental operating conditions for our present measurements and analysis methods were described in our Er paper (VIII). We shall, therefore, restrict this discussion to features mainly relating to the Yb measurements and analysis.

The separated isotope samples were obtained on loan from the Isotope Division at Oak Ridge. They were of the chemical form Yb_2O_3, with two or more pieces of 32×63-mm area packaged in thin Al foil, and using a small amount of diluted polystyrene cement for binder.

The transmission measurements mainly utilized our 200-m flight path ($E \gtrsim 25$ eV) supplemented by 40-m-path measurements extending down to ~1 eV. The isotope measurements used a 32×127-mm transmission aperture just outside the main cyclotron shield wall. For the transmission measurements the detectors were (thin) rectangular ^{10}B slabs intercepting the neutron flux, viewed by NaI (200-m) or plastic (40-m) γ-ray scintillation detectors which detect the (prompt) 480-keV γ rays associated with neutron capture in ^{10}B. The self-indication measurements used only the 40-m detector (described in VIII). For "D only" a sample was placed in the neutron flux at the center of the detector and capture γ rays in the sample were detected. The "$D+T$" measurements used both a "D" sample and another "T" sample of the same material at the transmission position. The conditions (resolution etc.) were essentially the same as for the Er measurements (VIII). The natural Yb samples had 76×254-mm area in a range of thicknesses. The thickest sample was of Yb metal. The pertinent sample thickness properties are summarized in Table I.

III. RESONANCE PARAMETER EVALUATION AND RESULTS

As discussed in the Er paper (VIII), we utilize transmission dip information at each resonance, for each sample thickness, to generate sets of implied ($g\Gamma_n$ vs Γ) curves. We also made some use of partial shape analysis at lower energies to supplement the area analysis. Also, for the odd-A isotopes, an independent self-indication data analysis after considering multiple-scattering interactions[6] yields further implied $g\Gamma_n$ vs Γ relations. Where the different $g\Gamma_n$ vs Γ curves for a given level intersect with a not too small angle between them, both $g\Gamma_n$ and Γ are separately determined. When this does not occur, we use $\Gamma \approx \langle\Gamma_\gamma\rangle + \Gamma_n$ to establish an intersection $g\Gamma_n$ value with the data-analysis curves. For even-even nuclei, $g=1$. For the ^{171}Yb, $I=\frac{1}{2}$, so $g=\frac{1}{4}$ or $\frac{3}{4}$ for $J=0$ or 1 compound-nucleus spin. For ^{173}Yb, $I=\frac{5}{2}$, so $g=\frac{5}{12}$ or $\frac{7}{12}$ for $J=2$ or 3, respectively. For these odd-A nuclei, the two curves for implied $\Gamma=\langle\Gamma_\gamma\rangle+\Gamma_n$ may be sufficiently different for the two possible J values, that a "best choice J" can be chosen if the analysis independently yields a best ($g\Gamma_n$, Γ) intersection point. In fact, however, the "D only" self-indication measurements, using the concept of an "absolute-saturation" count rate (if all neutrons were captured) gave a more sensitive distinction between the two J values with no need to use $\Gamma_\gamma \approx \langle\Gamma_\gamma\rangle$. Many resonance J values are obtained for these odd-A isotope resonances.

Examples of the resonance parameter analysis are given in Figs. 1(a)–1(d). Figures 1(a) and 1(b) for ^{171}Yb and ^{173}Yb are for levels where a particularly large number of separate, independent $g\Gamma_n$ vs Γ analysis curves give a good intersection for one value of J, but not the other possible J value. The (+) or (−) on the D only self-indication α and β curves are for $J=I+\frac{1}{2}$ and $I-\frac{1}{2}$, respectively. The text of the figures is self-explanatory. Figure 1(c) for ^{172}Yb and Fig. 1(d) for ^{174}Yb show cases of agreement for two or three independent Γ_n vs Γ analysis curves, and also with $\Gamma \approx \langle\Gamma_\gamma\rangle + \Gamma_n$. Figure 2 shows a shape fit to the same ^{174}Yb reso-

TABLE I. Parameters for the separated-ytterbium isotope and the natural-ytterbium samples. The samples are in the form Yb_2O_3.

	1/n (b/atom)						
Sample	Yb (all)	170	171	172	173	174	176
^{171}Yb	261	41100	296	3230	20900	18000	78900
^{171}Yb	522	82200	592	6460	41800	36000	158000
^{172}Yb	153	101000	5930	167	4450	7670	56000
^{173}Yb	156	96000	23400	4570	184	1540	30600
^{173}Yb	201	123000	30000	5870	236	1980	39300
^{173}Yb	708	435000	106000	20700	832	6980	139000
^{174}Yb	1420	870000	212000	41400	1660	14000	277000
^{176}Yb	78.6	154000	18900	7860	3560	82·1	14000
Nat.Yb[a]	119	230000	36100	22300	20900	5540	123
Nat.Yb	24.1	782	166	110	149	76·4	194
Nat.Yb	92	2980	634	418	569	292	740
Nat.Yb	138	4480	953	628	855	448	1110
Nat.Yb	276	8950	1900	1250	1710	874	2220

[a] This sample is in the form of metal.

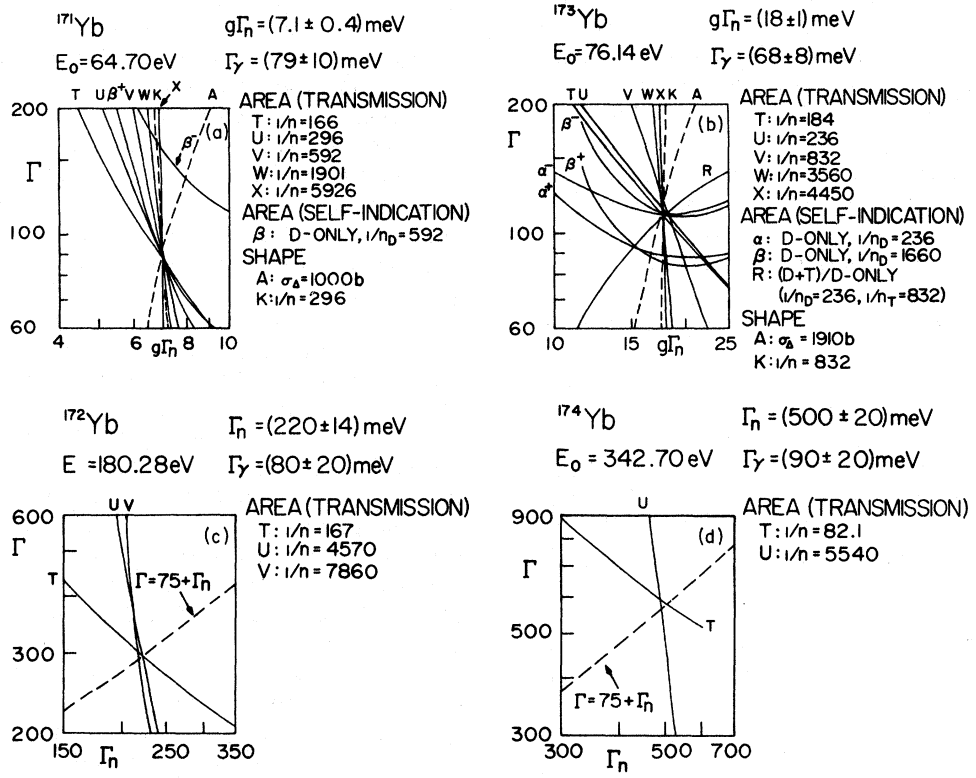

FIG. 1. (a) The ($g\Gamma_n$, Γ) curves implied from various analyses for the 64.7-eV level in ^{171}Yb. Curves T, U, V, W, and X are from transmission dip areas for successively decreasing sample thicknesses. Curve V is from 40-m data. The others are from 200-m data. Curve A is from the 200-m-data peak resonance cross-section value. Curve K is from a partial shape analysis of the 200-m transmission curve for the thickest sample. β^- and β^+ for $J = I - \frac{1}{2}$ and $I + \frac{1}{2}$, use the "absolute saturation" D only (self-indication detector) implied rate and the area of the "D only" count peak for this level. The $J = I + \frac{1}{2}$ fit is favored. The scales for Γ_n and Γ are in meV. (b) Similar analysis for the 76.14-eV level in ^{173}Yb. Curves T, U, V, W, and X are from the transmission dip area of the resonance for different sample thicknesses. Curves A, K, β^-, and β^+ are as for (a), while α^- and α^+ are similar to β^- and β^+ but for a different "D only" sample thickness. R is from the ratio of "$D + T$" to "D only" self-indication resonance count areas. We favor $J = I - \frac{1}{2}$. (c) Analysis curves based on the transmission dip areas for three samples, for the 180.28-eV level in ^{172}Yb. (d) Analysis curves for the 342.70-eV level in ^{174}Yb using transmission dip areas (two samples).

nance at 342.7 eV as in Fig. 1(d), where the asymmetry permits a separate evaluation of the scattering length R', appropriate for this level. We obtain $R' = 7.9 \pm 0.5$ fm.

The level energies and resonance reduced neutron widths, Γ_n^0 (or $g\Gamma_n^0$), are given in Tables II to VI for isotopes 171, 172, 173, 174, and 176, respectively, treating all levels as s levels. The cases where extra level parameter information was obtained, Γ_γ values or the level J values (171 or 173), are listed separately in Table VII. The measured average Γ_γ values are 76.5 meV for ^{171}Yb, 73.8 meV for ^{173}Yb, and 72.3 meV for the three levels of ^{172}Yb for which Γ_γ were obtained. The Γ_γ values are all consistent with a true mean $\approx$75 meV. The observed fluctuations in the individual Γ_γ values are probably mainly due to our experimental measurement uncertainties. Table VIII gives the results for levels attributed to isotopes 168 or 170 seen in the natural Yb sample. The assignment of two of the levels to ^{168}Yb (0.14% natural abundance) is mainly because they were not seen in the ^{170}Yb data of Mughabghab and Chrien.[5] A spectroscopic analysis by Lucius Pitkin, Inc. of the thick Yb metal sample shows no evidence for other rare earths, or other elements which could contribute one or more of the levels which we attribute to ^{168}Yb or ^{170}Yb. An independent search of the positions of strong level in possible contaminant nuclei also failed to yield any suspicious cases.

The "measured σ vs E" values near resonances

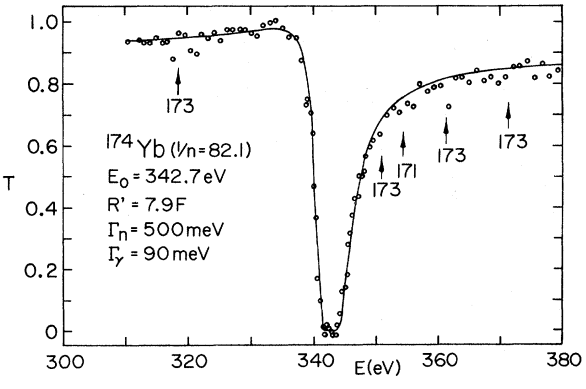

FIG. 2. Result of a shape fit to the transmission data for the ^{174}Yb level at 342.7 eV using a Breit-Wigner single-level formula with the indicated parameters. The formula included the Doppler effect and the $(E)^{1/2}$ variation of Γ_n with E. The interference asymmetry permitted a separate evaluation of R', giving $R' = 7.9 \pm 0.5$ fm. The arrows shown in the figure indicate the positions of the levels due to other Yb isotope impurities in the sample having ^{174}Yb as main isotope.

do not give a good approximation of the "true" behavior for reasons which we have repeatedly emphasized in our previous papers. Our deduced level parameters should be used to reconstruct the true resonance σ vs E. There is, however, some additional interest in the "between resonance" cross-section behavior.

The use of our thick Yb metal sample permits us to obtain the total natural Yb cross-section behavior between levels as shown in Fig. 3. We obtained this plot by using many channel averaging to reduce the statistical uncertainty spread in the individual points. To eliminate near resonance contributions, each particular many channel average is included only if the separate T (transmission) values for the included channels are all within a small enough spread from their mean and are not individually too low. Lines connect the points in the figure if there are no rejected regions between them (due to levels). Note that the right-hand vertical scale applies for natural Yb.

One obvious feature of interest in Fig. 3 is the steady increase in σ as E decreases below ~100 eV. This increase was found to be due mainly to the ^{174}Yb content (31.84%) in natural Yb. For comparison, we also show the similar σ vs E curve for ^{174}Yb using our thickest ^{174}Yb sample. This has been plotted so the scales are the same for $E > 200$ eV or $\sigma < 8$ b. For $E < 200$ eV, the left vertical scale applies for ^{174}Yb. It is the same as the natural Yb right scale for $\sigma \leq 8$ b, but increases 3 times as fast for $\sigma > 8$ b. Since ^{174}Yb comprises about $\frac{1}{3}$ of natural Yb, the increase in σ above ~8 b for natural Yb should be about $\frac{1}{3}$ as large as for ^{174}Yb. This is seen to be essentially true.

The lowest positive energy level in ^{174}Yb is that shown in Fig. 2 at 343 eV. The increase in σ below 100 eV is presumably due to one or more negative energy levels in ^{174}Yb. If one attempts to achieve a fit using a single dominant level at (negative) $E = E_0$, having parameters Γ_n^0 and Γ_γ, the energy scale of the drop-off of the cross section mainly establishes E_0. The thermal capture cross section, if due mainly to this level, determines $\Gamma_\gamma \Gamma_n^0 / E_0^2$, while the resonance part of the thermal scattering cross section depends on $(\Gamma_n^0)^2 / E_0^2$. Our σ vs E for ^{174}Yb is shown in Fig. 4. Using $\Gamma_\gamma = 75$ meV and $R' = 7.9$ fm, a best fit yields $E_0 = -20$ eV and $\Gamma_n^0 = 129$ meV. This predicts a thermal capture, σ, of 99 b, vs a reported[5] measured value of 65 b. The predicted total thermal cross section is 163 b (excluding paramagnetic scattering). This compares with the reported measured value of 137 b.[5] A choice $E_0 = -25$ eV, $\Gamma_n^0 = 160$ meV, $\Gamma_\gamma = 65$ meV, $R' = 7.5$ fm, gives agreement with the reported thermal σ_c and σ_{sc} but a little poorer fit to our σ vs E curve. In view of the thinness of our ^{174}Yb

TABLE II. Resonance parameters of ^{171}Yb (also, see Table VII).

E_0 (eV)	$g\Gamma_n^0$ (meV)	E_0 (eV)	$g\Gamma_n^0$ (meV)	E_0 (eV)	$g\Gamma_n^0$ (meV)
7.91±0.02	0.57 ±0.04	455.16±0.68	0.19 ±0.09	981.42±1.08	0.096±0.064
13.04±0.03	0.66 ±0.06	459.25±0.27	1.03 ±0.19	991.11±0.43	7.0 ±1.3
21.72±0.06	0.027±0.002	470.78±0.28	1.38 ±0.14	1005.3 ±0.5	0.79 ±0.19
28.13±0.04	0.32 ±0.02	483.62±0.29	1.05 ±0.14	1009.7 ±0.5	3.7 ±0.6
34.54±0.05	0.61 ±0.04	494.27±0.31	3.2 ±0.5	1017.5 ±0.5	1.76 ±0.31
41.36±0.06	1.17 ±0.06	499.12±0.31	3.6 ±0.5	1020.2 ±1.1	0.19 ±0.09
46.38±0.07	0.11 ±0.01	515.86±0.32	4.1 ±0.4	1026.9 ±0.5	2.8 ±0.4
52.87±0.09	0.69 ±0.04	524.80±0.33	2.8 ±0.3	1037.1 ±0.5	0.87 ±0.16
54.07±0.10	2.11 ±0.14	531.47±0.86	0.191±0.065	1047.9 ±0.5	0.53 ±0.19
60.09±0.05	0.54 ±0.03	538.90±0.34	10.3 ±1.3	1049.8 ±0.5	1.88 ±0.43
64.70±0.06	0.88 ±0.05	547.05±0.35	1.71 ±0.26	1062.9 ±0.5	2.1 ±0.4
76.94±0.08	1.11 ±0.08	557.67±0.92	0.097±0.042	1071.5 ±0.5	3.5 ±0.6
82.23±0.08	0.29 ±0.02	560.90±0.93	0.072±0.034	1078.7 ±0.5	0.49 ±0.15
84.31±0.09	0.26 ±0.02	577.74±0.38	1.8 ±0.2	1086.5 ±0.5	0.21 ±0.12
96.05±0.11	0.29 ±0.02	594.24±0.40	0.78 ±0.12	1091.4 ±0.5	1.03 ±0.21
107.61±0.12	3.7 ±0.2	598.23±0.40	1.23 ±0.20	1110.4 ±0.5	1.2 ±0.2
112.10±0.13	1.51 ±0.09	603.88±0.41	2.6 ±0.4	1136.2 ±0.5	6.2 ±1.2
120.24±0.15	0.011±0.006	612.50±0.42	1.7 ±0.2	1157.9 ±0.6	2.6 ±0.5
127.57±0.16	1.35 ±0.11	620.46±0.42	0.96 ±0.16	1167.1 ±0.6	1.2 ±0.3
139.92±0.18	1.01 ±0.25	628.58±0.43	2.4 ±0.3	1173.2 ±0.6	1.49 ±0.32
145.90±0.20	0.65 ±0.05	633.13±0.44	1.83 ±0.24	1185.9 ±0.6	0.70 ±0.23
160.41±0.23	5.0 ±0.4	648.90±0.45	1.1 ±0.2	1209.7 ±0.6	3.0 ±0.5
164.61±0.23	3.0 ±0.2	657.20±1.18	0.34 ±0.14	1217.2 ±0.6	0.57 ±0.17
175.61±0.13	0.83 ±0.08	661.76±0.47	2.3 ±0.4	1229.5 ±0.6	0.71 ±0.14
179.10±0.13	0.070±0.034	667.39±0.47	1.47 ±0.23	1234.8 ±0.6	0.17 ±0.09
182.29±0.14	0.84 ±0.10	673.57±0.48	0.56 ±0.10	1241.4 ±0.6	0.79 ±0.20
193.57±0.15	0.33 ±0.07	685.70±0.49	0.80 ±0.15	1251.0 ±0.6	6.5 ±1.1
208.30±0.17	0.35 ±0.07	691.63±0.50	1.52 ±0.23	1262.0 ±0.6	5.3 ±1.1
210.37±0.17	6.9 ±1.9	695.13±0.50	0.29 ±0.08	1269.3 ±0.6	2.1 ±0.5
216.80±0.23	0.047±0.025	709.40±0.52	6.6 ±0.8	1283.2 ±0.6	5.4 ±0.9
226.81±0.19	1.39 ±0.13	716.26±1.34	0.052±0.030	1290.8 ±0.6	6.7 ±1.1
239.88±0.21	0.23 ±0.05	731.09±0.54	1.92 ±0.22	1299.4 ±0.7	5.3 ±1.1
250.06±0.22	1.52 ±0.19	741.01±1.41	0.15 ±0.07	1322.1 ±0.7	4.7 ±0.8
255.26±0.23	1.82 ±0.25	746.20±0.56	0.66 ±0.11	1334.0 ±0.7	3.7 ±1.1
269.72±0.31	0.06 ±0.03	761.15±1.47	0.145±0.072	1352.3 ±1.7	0.19 ±0.11
276.60±0.25	0.50 ±0.08	774.90±0.59	0.97 ±0.14	1368.6 ±0.7	2.8 ±0.6
287.49±0.27	1.00 ±0.12	785.20±1.54	0.28 ±0.09	1377.7 ±0.7	1.32 ±0.43
290.58±0.27	4.8 ±0.4	790.79±0.61	3.5 ±0.5	1397.9 ±0.7	0.32 ±0.16
302.32±0.29	1.12 ±0.17	800.32±0.62	3.9 ±0.4	1437.6 ±0.7	4.6 ±1.2
310.10±0.30	1.82 ±0.23	810.80±0.81	0.070±0.035	1450.3 ±0.8	1.76 ±0.58
314.02±0.31	0.17 ±0.07	817.64±0.64	1.54 ±0.17	1453.4 ±0.8	1.91 ±0.66
319.89±0.31	1.40 ±0.22	829.35±0.33	0.63 ±0.07	1461.7 ±0.8	2.2 ±0.6
333.05±0.32	0.17 ±0.08	838.57±0.33	0.69 ±0.10	1469.4 ±0.8	0.83 ±0.29
341.61±0.35	0.87 ±0.16	841.56±0.34	1.96 ±0.21	1481.0 ±0.8	4.2 ±0.8
344.40±0.35	1.72 ±0.27	851.50±0.34	0.48 ±0.07	1499.1 ±0.8	3.9 ±0.8
354.41±0.37	8.8 ±1.3	875.25±0.36	2.9 ±0.4	1516.9 ±0.8	3.1 ±0.5
359.45±0.48	0.17 ±0.08	896.15±0.37	4.7 ±0.7	1524.4 ±0.8	1.15 ±0.38
370.41±0.50	0.125±0.062	905.39±0.38	1.33 ±0.17	1534.7 ±0.8	5.4 ±1.0
382.15±0.52	0.138±0.051	915.53±0.38	0.76 ±0.17	1549.6 ±0.9	1.3 ±0.5
387.21±0.42	6.9 ±1.3	923.54±0.39	2.5 ±0.4	1586.9 ±0.9	4.8 ±1.3
391.99±0.54	0.18 ±0.09	927.00±0.39	5.3 ±0.8	1593.8 ±0.9	0.98 ±0.38
409.39±0.46	0.77 ±0.12	932.43±0.39	3.7 ±0.6	1617.6 ±0.9	2.4 ±0.7
411.67±0.46	0.94 ±0.15	938.68±0.40	1.24 ±0.33	1637.3 ±0.9	1.43 ±0.49
434.57±0.25	2.06 ±0.24	945.01±0.40	1.82 ±0.23	1661.6 ±0.9	2.9 ±1.0
436.68±0.25	0.60 ±0.14	962.36±1.05	0.42 ±0.16	1675.8 ±0.9	1.17 ±0.37
444.78±0.26	2.9 ± 0.3	971.82±1.06	0.19 ±0.10	1684.7 ±0.9	3.4 ±0.7

sample, and certain other experimental difficulties of establishing proper background subtractions at extreme low energy, our measured σ values have some systematic uncertainty in this region. The solution using $E_0 = -25$ eV is, therefore, recommended.

IV. SYSTEMATICS OF THE RESULTS–COMPARISON WITH THEORY

Figures 5(a) and 5(b) show the cumulative level count, N vs E for the odd isotopes (171 and 173) and Figs. 5(c)–5(e) for the even isotopes (172, 174, and 176). The odd-A isotopes each have two independent s level populations corresponding to $J = I \pm \frac{1}{2}$. They also have much smaller mean level spacings. Since the Wigner level repulsion does not apply between levels of different J, we expect to begin to miss s levels starting at a much lower energy for the odd isotopes than for the even isotopes. Both ^{171}Yb and ^{173}Yb show a higher N vs E initial slope, followed by a larger interval of smaller, but still very nearly linear slope behavior, followed by an eventual pronounced drooping of the slope for ^{171}Yb at the highest energies. From other evidence we believe that essentially no p levels are included in these populations, so the decreased slope is due to missing s levels. The initial higher slope gives more closely the true s level mean spacing $\langle D \rangle$.

The N vs E histogram for ^{172}Yb is quite linear to 4 keV, with evidence for an increasing fractional level loss above 4 keV. The failure to see any ^{172}Yb levels in the 500-eV-wide interval 6.0 to 6.5 keV seems to indicate that only weak (missed) s levels exist in this interval.

The ^{174}Yb histogram of N vs E is linear to 3.3 keV, with evidence of increasing loss of levels above this energy. The similar histogram for ^{176}Yb gives a straight line, with >0 intercept, to about 3.9 keV, followed by increasing level loss at higher energies. There is some reason to sus-

TABLE III. Resonance parameters of ^{172}Yb (also, see Table VII).

E_0 (eV)	Γ_n^0 (meV)	E_0 (eV)	Γ_n^0 (meV)	E_0 (eV)	Γ_n^0 (meV)
139.82±0.18	11.3 ±0.7	2433.4±1.7	1.26±0.81	5371.8±2.7	7.2±1.5
180.28±0.13	16 ±1	2520.9±0.9	7.2 ±1.2	5565.6±2.9	25 ±4
201.48±0.16	0.92±0.08	2549.1±0.9	3.0 ±0.8	5631.5±2.9	4.9±1.6
323.68±0.32	0.34±0.03	2574.8±0.9	41 ±6	5654.7±2.9	57 ±9
459.25±0.27	1.87±0.23	2726.7±1.0	31 ±6	5775.9±3.0	6.4±1.7
508.72±0.32	12.4 ±0.9	2817.8±1.0	4.7 ±0.9	5830.4±3.0	6.9±1.7
544.42±0.35	1.03±0.17	2901.7±1.1	8.4 ±1.3	5904.2±3.1	23 ±4
619.62±0.43	3.7 ±0.3	2913.5±1.1	17.6 ±2.6	5949.5±3.2	9.5±2.6
661.99±0.47	2.1 ±0.3	2953.1±1.1	13.2 ±1.8	6534.3±3.6	7.3±1.5
753.79±0.57	30 ±2	3027.8±1.2	12.9 ±1.6	6588.8±3.7	34 ±6
815.40±0.64	7.4 ±0.9	3100.6±1.2	3.5 ±1.1	6610.8±3.7	10 ±2
859.19±0.35	0.96±0.17	3203.2±1.3	10.8 ±1.4	6791.5±3.5	9.3±1.9
875.61±0.36	2.3 ±0.3	3238.1±1.3	23 ±3	6876.6±3.9	11.9±1.8
981.37±0.42	0.73±0.16	3334.8±1.3	5.2 ±1.4	7086.2±4.1	13 ±2
1066.7 ±0.5	10 ±1	3385.5±1.4	0.64±0.41	7154.0±4.2	43 ±5
1129.4 ±0.5	1.25±0.21	3520.2±1.4	9.1 ±1.7	7267.1±4.3	52 ±8
1204.0 ±0.6	0.55±0.20	3556.2±1.5	19 ±3	7435.3±4.4	27 ±3
1282.3 ±0.7	1.06±0.34	3695.1±1.5	27 ±3	7515.0±4.5	28 ±3
1334.7 ±0.7	2.7 ±0.4	3734.6±1.6	4.3 ±0.8	7666.6±4.6	48 ±7
1455.6 ±0.8	2.5 ±0.4	3813.1±1.6	12.3 ±1.5	7799.2±4.7	20 ±6
1511.9 ±0.8	7.5 ±0.8	3878.4±1.7	6.3 ±1.3	8060.1±5.0	8.4±2.5
1702.8 ±0.5	0.27±0.17	3900.0±1.7	3.5 ±1.3	8221.0±5.1	17 ±3
1733.9 ±0.5	5.5 ±0.7	4022.9±1.8	2.7 ±0.9	8298.0±5.2	33 ±5
1786.8 ±0.5	7.3 ±1.2	4205.4±1.9	6.3 ±1.4	8601.0±5.5	11 ±3
1826.6 ±1.0	108 ±16	4362.8±2.0	14 ±2	8705.6±5.6	34 ±6
1892.7 ±0.6	23 ±4	4386.5±2.0	14 ±2	9132.1±6.0	24 ±4
1914.8 ±0.6	25 ±4	4483.6±2.1	11.2 ±1.6	9223.1±6.1	59 ±8
1977.4 ±0.6	0.45±0.31	4566.9±2.1	3.6 ±0.9	9476.7±6.4	8.2±4.1
2001.6 ±0.7	0.72±0.51	4685.3±2.2	8.6 ±2.1	9656.0±6.5	45 ±8
2120.3 ±0.7	10.8 ±1.7	4837.1±2.3	4.2 ±0.9	9767.4±6.6	34 ±7
2162.1 ±0.7	2.1 ±0.5	4877.6±2.3	86 ±13	9807.2±6.6	13 ±5
2278.7 ±0.8	0.78±0.25	5001.1±2.5	20 ±4	9927.9±6.8	31 ±7
2401.4 ±0.8	98 ±14	5273.5±2.6	44 ±7	10017 ±7	30 ±7
				10102 ±7	16 ±5

TABLE IV. Resonance parameters of ^{173}Yb (also, see Table VII).

E_0 (eV)	$g\Gamma_n^0$ (meV)	E_0 (eV)	$g\Gamma_n^0$ (meV)	E_0 (eV)	$g\Gamma_n^0$ (meV)
4.51±0.02	0.052±0.005	565.58±0.94	0.063±0.029	1162.3±0.6	2.3 ±0.4
17.63±0.04	3.1 ±0.2	574.90±0.38	0.25 ±0.06	1169.6±0.6	3.5 ±0.5
31.39±0.08	6.4 ±0.4	588.84±1.00	0.21 ±0.12	1185.3±0.6	6.4 ±0.9
35.72±0.05	3.8 ±0.2	593.86±1.01	0.28 ±0.11	1195.5±0.6	4.5 ±0.9
45.16±0.07	2.2 ±0.2	605.51±0.41	3.5 ±0.4	1199.4±0.6	3.6 ±0.8
53.47±0.09	0.52 ±0.04	618.77±0.42	3.7 ±0.5	1205.1±0.6	3.1 ±0.8
58.88±0.05	0.52 ±0.04	621.31±0.43	0.24 ±0.12	1209.7±0.6	1.7 ±1.0
66.18±0.06	0.52 ±0.04	648.45±0.45	2.2 ±0.3	1212.0±0.6	0.83±0.83
68.91±0.06	0.51 ±0.04	653.91±0.46	0.36 ±0.08	1217.2±0.6	0.57±0.29
74.49±0.07	0.41 ±0.05	659.44±0.46	0.74 ±0.12	1235.4±0.6	3.3 ±0.7
76.14±0.07	2.1 ±0.1	682.65±0.49	0.153±0.077	1241.1±0.6	2.9 ±0.6
96.42±0.10	0.60 ±0.05	690.14±0.50	1.41 ±0.19	1258.6±0.6	0.85±0.34
105.75±0.12	2.9 ±0.2	701.70±0.51	1.81 ±0.23	1263.5±0.6	4.2 ±0.8
111.07±0.13	0.59 ±0.05	705.28±0.51	0.94 ±0.15	1274.9±0.6	0.62±0.31
115.15±0.14	0.013±0.005	710.93±1.33	0.038±0.023	1309.7±0.6	0.86±0.28
124.32±0.15	0.90 ±0.05	721.65±0.53	0.20 ±0.07	1313.6±0.7	0.24±0.12
128.84±0.16	3.1 ±0.2	728.93±0.54	4.6 ±0.6	1354.2±0.7	2.3 ±0.4
134.81±0.17	0.35 ±0.03	766.41±0.58	2.5 ±0.3	1368.2±0.7	3.6 ±0.6
145.33±0.19	0.80 ±0.07	771.37±0.59	0.43 ±0.11	1374.9±0.7	1.7 ±0.4
154.15±0.21	0.077±0.010	774.02±0.59	1.33 ±0.22	1381.2±0.7	2.4 ±0.5
155.73±0.21	0.136±0.016	782.34±0.60	1.64 ±0.22	1406.1±0.7	0.93±0.21
168.81±0.24	2.2 ±0.2	789.83±1.55	0.18 ±0.07	1422.8±0.7	0.45±0.24
197.31±0.15	1.07 ±0.11	796.30±0.62	0.52 ±0.09	1436.9±0.8	1.85±0.55
204.96±0.16	0.26 ±0.03	811.91±0.64	0.17 ±0.07	1440.6±0.8	0.50±0.26
210.20±0.17	0.54 ±0.05	815.08±0.64	0.49 ±0.14	1443.6±0.8	0.74±0.39
221.67±0.18	0.28 ±0.03	846.59±0.34	2.2 ±0.3	1448.1±0.8	0.76±0.39
226.44±0.19	0.25 ±0.03	850.99±0.34	3.8 ±0.5	1454.1±0.8	3.3 ±0.7
229.64±0.19	0.96 ±0.07	864.90±0.35	4.2 ±0.4	1464.8±0.8	0.44±0.26
250.60±0.22	2.5 ±0.2	883.09±0.36	0.25 ±0.06	1471.7±0.8	3.0 ±0.6
256.60±0.23	0.91 ±0.09	891.40±0.37	0.55 ±0.08	1480.3±0.8	3.0 ±0.6
277.36±0.25	0.75 ±0.08	895.78±0.37	1.47 ±0.23	1498.3±0.8	5.4 ±1.0
283.53±0.26	2.4 ±0.2	925.84±0.39	7.9 ±1.3	1518.3±0.8	5.9 ±1.0
286.43±0.27	0.51 ±0.07	932.04±0.39	0.28 ±0.08	1537.9±0.8	0.61±0.31
303.94±0.37	0.034±0.023	937.11±0.40	1.24 ±0.20	1549.6±0.9	0.81±0.41
307.13±0.29	5.7 ±0.4	941.25±0.40	1.86 ±0.29	1566.4±0.9	3.3 ±0.8
318.33±0.31	1.21 ±0.11	958.46±0.41	2.4 ±0.3	1569.8±0.9	3.5 ±0.8
324.00±0.32	0.34 ±0.04	968.47±0.41	2.2 ±0.3	1582.6±0.9	0.96±0.30
340.06±0.34	1.14 ±0.16	973.85±0.42	0.99 ±0.16	1593.8±0.9	1.25±0.40
351.14±0.36	0.57 ±0.06	985.80±0.43	0.25 ±0.10	1617.6±0.9	9.2 ±1.5
361.45±0.38	2.7 ±0.3	993.25±0.43	1.75 ±0.51	1631.0±0.9	1.26±0.40
371.24±0.39	0.93 ±0.10	997.97±0.43	7.0 ±1.3	1641.0±0.9	0.64±0.32
392.47±0.43	0.121±0.025	1008.8 ±0.4	4.4 ±0.7	1679.6±0.5	0.88±0.34
405.06±0.45	0.094±0.030	1017.5 ±0.5	2.1 ±0.4	1684.3±0.5	1.07±0.37
420.05±0.23	2.7 ±0.3	1022.4 ±0.5	1.41 ±0.28	1698.5±0.5	0.46±0.17
429.77±0.25	0.55 ±0.08	1027.4 ±0.5	0.24 ±0.09	1704.7±0.5	2.3 ±0.5
438.94±0.25	4.3 ±0.5	1044.2 ±0.5	0.65 ±0.15	1711.5±0.5	0.31±0.17
447.62±0.26	2.5 ±0.3	1061.0 ±0.5	0.27 ±0.07	1720.7±0.5	0.77±0.27
460.33±0.27	0.37 ±0.06	1069.1 ±0.5	4.0 ±0.6	1730.9±0.5	5 ±1
488.16±0.30	4.3 ±0.5	1079.0 ±0.5	1.58 ±0.24	1739.8±0.5	2.3 ±0.7
497.24±0.31	0.135±0.045	1086.5 ±0.5	0.82 ±0.15	1748.8±0.5	0.45±0.22
514.42±0.32	1.94 ±0.22	1107.4 ±0.5	1.41 ±0.21	1755.8±0.5	0.24±0.14
528.44±0.33	1.00 ±0.17	1118.1 ±0.5	1.47 ±0.21	1760.8±0.5	0.43±0.21
547.57±0.35	4.0 ±0.4	1137.0 ±0.5	0.80 ±0.21	1775.8±0.5	2.9 ±0.6
550.06±0.36	2.2 ±0.3	1140.9 ±0.5	2.5 ±0.4	1782.7±0.5	3.9 ±0.8
557.16±0.36	0.17 ±0.04	1153.1 ±0.5	0.29 ±0.15	1789.9±0.5	1.02±0.38
				1796.8±0.5	0.99±0.26

TABLE V. Resonance parameters of ^{174}Yb (also, see Table VII).

E_0 (eV)	Γ_n^0 (meV)	E_0 (eV)	Γ_n^0 (meV)	E_0 (eV)	Γ_n^0 (meV)
342.70±0.35	27.5 ±1.6	5218.9±2.6	82 ±12	11392± 9	18.7± 3.7
585.42±0.39	5.0 ±0.5	5369.1±2.7	4.4±1.0	11501± 9	53 ± 9
880.23±0.36	19.2 ±1.3	5653.2±2.9	106 ±13	11759± 9	31 ± 6
1002.7 ±0.4	7.9 ±0.8	5752.0±3.0	14.5±2.6	12025± 9	12.8± 4.1
1179.8 ±0.6	1.22±0.20	5954.2±3.2	18.1±2.6	12528±10	22 ± 6
1301.3 ±0.7	26 ±2	6333.0±3.5	4.1±0.9	12722±10	98 ±18
1634.6 ±0.9	0.32±0.20	6503.6±3.6	2.4±0.9	13196±11	70 ±14
1668.6 ±1.0	186 ±24	6718.8±3.8	16.3±2.7	13450±11	119 ±17
1738.8 ±0.5	19.2 ±3.4	7080.0±4.1	34 ±5	14406±12	119 ±17
1959.6 ±0.6	54 ±5	7519.4±4.5	12.2±2.9	14525±12	30 ± 7
2073.1 ±0.7	1.45±0.26	7726.6±4.7	100 ±11	14953±13	40 ± 8
2259.9 ±0.8	23 ±3	7851.3±4.8	5.6±1.5	15143±13	12.2± 2.4
2477.0 ±0.9	15.5 ±2.0	8104.9±5.0	9.2±2.2	15258±13	33 ± 7
2571.2 ±0.9	1.06±0.18	8689.0±5.6	56 ±9	15707±14	144 ±24
2620.4 ±0.9	66 ±8	8840.6±5.7	98 ±13	15829±14	74 ±14
2682.3 ±1.0	0.77±0.15	9389.0±6.2	12.1±2.6	16147±14	72 ±14
3058.1 ±1.2	13 ±2	9754.2±6.6	54 ±7	16431±15	82 ±16
3080.1 ±1.2	15.9 ±2.3	10017 ±7	23 ±4	17223±16	28 ±11
3287.7 ±1.3	70 ±9	10148 ±7	9.4±3.0	17568±16	43 ± 8
3540.3 ±1.5	23 ±3	10304 ±7	105 ±15	17810±17	69 ±15
3840.7 ±1.6	11 ±2	10405 ±7	10.8±2.9	18090±17	36 ±10
4036.9 ±1.8	14.3 ±1.7	10566 ±8	42 ±7	18207±17	33 ±10
4146.3 ±1.9	9.3 ±1.6	10694 ±8	46 ±8	18291±17	96 ±18
4482.6 ±2.1	33 ±4	10878 ±8	25 ±6	18600±18	40 ±15
4868.3 ±2.3	59 ±7	11003 ±8	75 ±15	18916±18	68 ±18
5149.6 ±2.5	3.1 ±0.7	11083 ±8	31 ±8	19801±19	33 ± 7

TABLE VI. Resonance parameters of ^{176}Yb.

E_0 (eV)	Γ_n^0 (meV)	E_0 (eV)	Γ_n^0 (meV)	E_0 (eV)	Γ_n^0 (meV)
97.88±0.11	0.055±0.006	3792.3±1.6	7.5± 1.0	9853.9± 6.7	90 ±12
148.45±0.20	0.80 ±0.06	4300.3±2.0	30 ± 3	10515 ± 7	16.6± 4.9
397.85±0.44	11 ±1	4351.0±2.0	18.2± 2.3	11629 ± 9	14.8± 4.6
488.30±0.60	118 ±5	4620.2±2.2	10.9± 1.5	11733 ± 9	83 ±13
726.00±1.07	148 ±7	5037.7±2.5	38 ± 4	12043 ± 9	13.7± 7.3
949.90±0.81	0.32 ±0.23	5382.6±2.7	94 ±11	12089 ± 9	10.0± 5.5
992.82±0.86	0.23 ±0.16	5481.3±2.8	8.6± 1.8	12432 ±10	108 ±15
1182.0 ±0.6	0.44 ±0.32	5716.3±3.0	320 ±40	12761 ±10	168 ±27
1392.5 ±0.7	51 ±4	6001.7±3.2	40 ± 5	13408 ±11	199 ±35
1571.5 ±1.7	151 ±15	6315.8±3.5	75 ±10	13601 ±11	159 ±26
1606.8 ±0.9	12 ±1	6480.4±3.6	7.7± 1.2	13732 ±11	179 ±26
1915.9 ±1.2	0.66 ±0.41	6722.6±3.8	52 ± 6	14051 ±12	75 ±12
2009.3 ±0.6	29 ±3	6955.3±4.0	80 ±10	14242 ±12	52 ±10
2180.1 ±0.7	64 ±6	7331.1±4.3	34 ± 5	15067 ±13	33 ± 8
2487.1 ±0.9	6.2 ±1.0	7555.2±4.5	10.6± 2.1	15169 ±13	101 ±16
2508.8 ±0.9	0.86 ±0.60	7801.5±4.7	16.4± 3.4	16077 ±44	30 ± 9
2722.4 ±1.0	8.6 ±1.3	8200.6±5.1	27 ± 3	17713 ±16	101 ±20
2929.1 ±1.1	166 ±18	8595.5±5.5	92 ±11	17794 ±16	97 ±22
3234.3 ±1.3	31 ±3	8739.1±5.6	36 ± 4	18156 ±17	85 ±15
3360.7 ±2.7	0.83±0.55	8984.6±5.9	95 ±11	18783 ±18	27 ± 9
3660.0 ±1.5	20 ±2	9217.0±6.1	60 ± 8	18988 ±18	65 ±16
3781.1 ±1.6	1.87±0.33	9495.7±6.4	280 ±30	19499 ±19	172 ±29
		9721.3±6.6	79 ±10	19649 ±19	150 ±25

pect that a few p levels were detected below 3.9 keV. This is discussed in more detail below.

The plots of $\sum\Gamma_n^0$ or $\sum g\Gamma_n^0$ vs E are given in Figs. 6(a)–6(f). These plots are much less sensitive to missed weak levels, and seem to be free of the drooping at higher energies seen in the N vs E plots. The average slopes of these plots determine the s level strength functions, S_0, for the isotopes. The value of $10^4S_0 = 1.86$ for ^{171}Yb has a long range consistency over the full-energy interval. The slope is significantly higher for the 900- to 1800-eV interval than for the 0-900-eV region for ^{173}Yb. This is shown by the three straight lines on Fig. 6(b). For $\langle D\rangle = 7.81$ eV for s levels, 115 levels per 900 eV, the two slopes (1.34 and 1.88) differ by about 34% of their mean, whereas the predicted statistical fractional rms difference for two equal intervals of 115 levels each is about 19%. This is not a very unlikely event.

Figure 6(c) for ^{172}Yb has a strange region of low slope to 1800 eV followed by the strongest of its levels at 1827 eV. The histogram subsequently stays close to the mean slope corresponding to $10^4S_0 = 1.68$. A similar low slope to 1600 eV is seen for ^{174}Yb [Fig. 6(d)], again followed by its strongest level which is at 1669 eV. The subsequent slope is reasonably close to the average $10^4S_0 = 1.62$. The ^{176}Yb histogram, Fig. 6(e), remains reasonably close to the mean slope $10^4S_0 = 2.29$, but appears to have a small superimposed oscillation of period ~4 keV. For the first 24 levels of ^{172}Yb to 1788 eV, the sample average Γ_n^0 is 5.38 meV, vs $\langle\Gamma_n^0\rangle = 11.8$ meV for our final choice S_0 and $\langle D\rangle$ for ^{172}Yb. For 24 uncorrelated Γ_n^0 values drawn from a single-channel Porter-Thomas (PT) distribution having the above $\langle\Gamma_n^0\rangle$, the probability[7] is ~1% that the 24 level sample Γ_n^0 value would be $\leq$ the observed value. Only 7 levels are involved for ^{174}Yb to 1640 eV where the average Γ_n^0 is so small, and this has ~15% probability of occurring for uncorrelated Γ_n^0 values drawn from a PT distribution having a $\langle\Gamma_n^0\rangle$ appropriate for the larger interval.

Figure 6(f) for ^{170}Yb is more difficult to treat owing to the large initial contribution of the strongest level at 40 eV and the effect of missed levels at higher energies. Our value $10^4S_0 = 2.25$ is to be considered to have a very large uncertainty associated with it, i.e., $10^4S_0 = 2.25 \pm 1.0$. The value $10^4S_0 = 2.46 \pm 0.67$ of Ref. 5 should be regarded as a better value, since a ^{170}Yb separated isotope sample was used.

The distribution histograms for $(g\Gamma_n^0)^{1/2}$ or $(\Gamma_n^0)^{1/2}$ are shown in Figs. 7(a)–7(e). In each case,

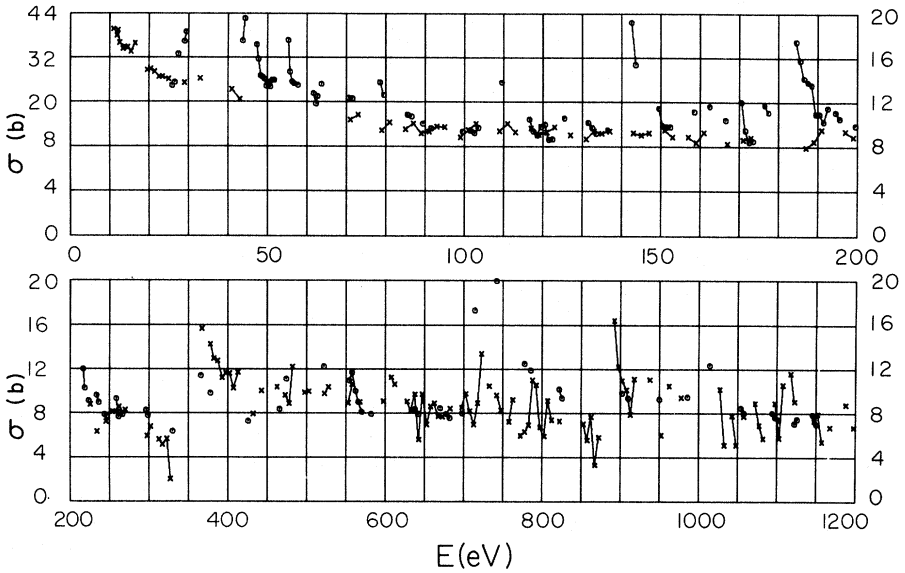

FIG. 3. The total "between resonance" cross section vs energy for natural Yb and for ^{174}Yb are denoted by ⊙ and ×, respectively. The natural Yb metal sample had $1/n = 24.1$ b/atom, while the ^{174}Yb oxide sample had $1/n = 82.1$ b/atom. Each experimental value is a many channel average satisfying test requirements that none of the individual transmission, T, values within the averaged group was below a certain value, or that the $(T_{max} - T_{min})$ within the average did not exceed a certain value (or the average was not used). If two adjacent averages were used, they were connected by a line. Below 200 eV the right scale is for natural Yb and the nonuniform left scale is for ^{174}Yb. Since the gradual increase in σ above 8 b for natural Yb is mainly due to its ^{174}Yb content (~$\frac{1}{3}$ abundance), the ^{174}Yb scale above 8 b increases 3 times as fast as the natural Yb scale. The rough agreement demonstrates the above point.

TABLE VII. Obtained Γ_γ values for ^{171}Yb, ^{173}Yb, ^{172}Yb and ^{174}Yb, and level J values (171 and 173) if also determined.

E_0 (eV)	Γ_γ (meV)	J	E_0 (eV)	Γ_γ (meV)	J	E_0 (eV)	Γ_γ (meV)
^{171}Yb			^{173}Yb			^{172}Yb	
7.91± 0.02	80±10		4.51±0.02	66± 8		139.82±0.18	77±16
13.04± 0.03	78±10		17.63±0.04	78± 9		180.28±0.13	80±20
28.13± 0.04	86±12		31.39±0.08	68± 8	2	508.72±0.32	60±20
34.54± 0.05	77± 8	0	35.72±0.05	84± 9	3		
41.36± 0.06	66± 8	0	45.16±0.07	76± 9		^{174}Yb	
52.87± 0.09	73±18	1	53.47±0.09	78±12			
54.07± 0.10	76±12	1	58.88±0.05	74±10			
60.09± 0.05	72±10	0	66.18±0.06	72±12		342.70±0.35	90±20
64.70± 0.06	79±10	1	68.91±0.06	69±14		585.42±0.39	76±20
76.94± 0.08	69±12	1	76.14±0.07	68± 8	2		
96.05± 0.11	59±18	0	96.42±0.10	75±15			
107.61± 0.12	80±12	1	105.75±0.12	70± 7	2		
112.10± 0.13	89±12	0	111.07±0.13	73±15			
127.57± 0.16	70±14	1	124.32±0.15	63±12			
160.41± 0.23	80±14	1	128.84±0.16	74± 9	3		
164.61± 0.23	70±10	1	145.33±0.19	64±15			
175.61± 0.13	69±15	1	168.81±0.24	72±10	3		
226.81± 0.19	74±10	1	197.31±0.15	77±18			
250.06± 0.22	84±12	1	229.64±0.19	58±14			
255.26± 0.23	100±20	1	250.60±0.22	70±10	3		
287.49± 0.27	80±18	1	256.60±0.23	85±15			
290.58± 0.27	86±20	1	277.36±0.25	72±14			
310.10± 0.30	80±15	0	283.53±0.26	62±12	3		
354.41± 0.37	82±14	1	307.13±0.29	95±12	2		
387.21± 0.42	70±25	0	318.33±0.31	83±15	3		
444.78± 0.26	80±14	1	340.06±0.34	76±10			
470.78± 0.28	72±15	1	351.14±0.36	74±10			
483.62± 0.29	62±18	1	371.24±0.39	69±17			
499.12± 0.31	78±15	1	438.94±0.25	66±14	3		
515.86± 0.32	80±20	1	447.62±0.26	58±15	3		
524.80± 0.33	77±18	1	488.16±0.30	89±15	3		
538.90± 0.34	70±15	0	514.42±0.32	100±22	2		
577.74± 0.38	72±15	1	547.57±0.35	78±15	3		
598.23± 0.40	87±18	1					
603.88± 0.41	73±16	1					
612.50± 0.42	64±16	1					
628.58± 0.43	86±20	1					

they are compared with single channel PT curves which are normalized to the experimental S_0 value, but where the total number of levels may differ from the observed number in any interval to correct for missed s levels, or possible (improperly) included p levels, or "noise levels." In each case, it was found that a better fitting could be made using a larger energy interval, even though a larger fraction of the levels were missed. It was assumed that the missed levels were the weaker levels, so the fits were made just to the part of the histogram containing the larger $(\Gamma_n^0)^{1/2}$ or $(g\Gamma_n^0)^{1/2}$ values. Since the missed weaker levels did not contribute significantly to the strength function, the PT curves all were for the measured S_0 values, with the total number of levels in each energy interval, N, treated as a fitting parameter. In each case, the best fit for the stronger levels suggested that many weaker levels had been missed. Note that we assume the correctness of the PT single channel distribution if a complete s population were involved for the energy interval, and we use the PT relation as a test of missed levels in the data.

The nearest neighbor level spacing distributions are shown in Figs. 8(a)–8(e). In this case, the histograms are restricted to the smaller energy intervals over which an initial linear slope was seen in Figs. 5(a)–5(e). The theoretical fit curves are for a single population Wigner distribution for the even isotopes, and for a mixed two population distribution for the odd-A cases. Relative level densities for the different J were taken in the ratio of the $(2J+1)$ values. For ^{171}Yb and ^{173}Yb the solid curves are for the observed number of levels while the dashed curve for ^{171}Yb is for larger numbers which we believe better reflect the true $\langle D \rangle$ value. The higher dashed histogram position in the first

histogram box shows the implied number of smallest spacings. Unfortunately, correction for each missed level divides one of the "observed" spacings into two parts, so it also influences the higher boxes. One may say that the over-all "corrected fit" to the Wigner curve is plausible, but not excellent, for ^{171}Yb.

The nearest neighbor level spacing histogram for ^{172}Yb, Fig. 8(c), is seen to be in excellent agreement with a single population Wigner curve. Similarly, Fig. 8(d) for ^{174}Yb shows a solid experimental histogram which corresponds to the observed spacing distribution. A dashed histogram having a better fit to the Wigner curve is also shown corresponding to the same number of levels, but with corrections to the s-level population. Figure 8(e) for ^{176}Yb similarly has a solid histogram for the observed spacing distribution and a "modified" distribution having two fewer levels. The methods of s population modification are described below.

Since the uncorrected ^{172}Yb level set to 3900 eV seems to agree well with the above tests, we also applied the Dyson-Mehta Δ_3 test,[8] which we call the "Δ test" and is that previously reported for Er and Sm. (Δ is the mean square deviation of a best-fit straight line from the N vs E histogram.) The comparison is shown in Fig. 9(a). The measured Δ of 0.41 is in excellent agreement with the Dyson-Mehta predicted value of 0.40 ± 0.11. A value $\rho = -0.24$ was obtained for the correlation coefficient for adjacent spacings, vs $\rho = -0.27 \pm 0.13$ expected from the O.E. theory. Figure 9(b) shows a plot, similar to those which we made for ^{166}Er and other cases (VIII). The plot gives the probability that a randomly measured $\Delta + \rho(S_j, S_{j+1}) \equiv \Delta + \rho$

TABLE VIII. Resonance parameters of ^{168}Yb and ^{170}Yb.

E_0 (eV)	Γ_n^0 (meV)
^{168}Yb	
22.50±0.04	6.1 ±0.4
188.09±0.28	12.5 ±2.6
^{170}Yb	
8.13±0.06[a]	0.583±0.053
39.93±0.06	30 ±4
66.57±0.06	5.2 ±2.0
72.91±0.07	6.3 ±1.1
95.31±0.10	1.43 ±0.41
167.7 ±2.0[a]	1.6 ±0.3
212.81±0.34	13 ±2
269.97±0.24	4.6 ±0.9
286.35±0.27	7.2 ±2.4
358.00±0.38	3.8 ±1.1
384.0 ±6.0[a]	3.3 ±1.0
394.0 ±7.0[a]	3.5 ±1.0
447.88±0.52	9.5 ±1.9
451.80±0.53	3.2 ±0.7
612.08±0.83	8.5 ±2.4
761.79±1.15	7.2 ±1.8
808.75±1.26	7.0 ±1.4
868.91±0.70	3.0 ±0.7
952.60±0.80	1.39 ±0.49
978.43±0.84	20 ±4
1037.1 ±1.0	6.8 ±2.5
1296.2 ±1.2	10.0 ±3.2
1328.0 ±1.4	5.2 ±1.4

[a] These levels are quoted from Ref. 5 for completeness.

TABLE IX. Summary of the "final choice" selections for the mean s-level spacings $\langle D \rangle$ and strength functions S_0. Indicated fractional uncertainties are calculated by $\pm 2.5/N$ (odd A) and $\pm 2/N$ (even A) for $\langle D \rangle$, and $(2/N)^{1/2}$ for S_0.

Isotope	$\langle D \rangle$ (eV)	$10^4 S_0$
170		2.25±1.0
171	5.79±0.48	1.86±0.16
172	70.3 ±2.6	1.68±0.20
173	7.81±0.93	1.60±0.28
174	162 ±18	1.62±0.21
176	185 ±19	2.29±0.32

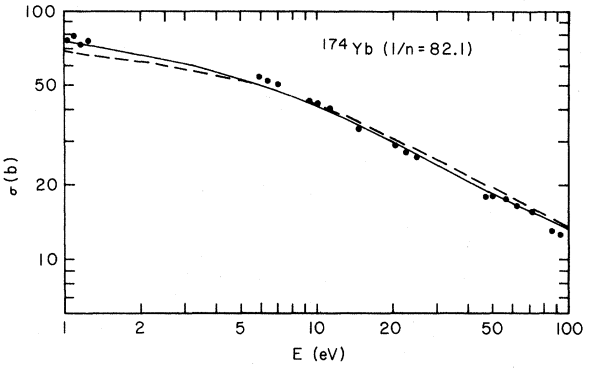

FIG. 4. A single bound level fit to the total cross sections of ^{174}Yb between 1 and 100 eV. The data points represent many channel averages where the cross sections are believed to be free of the influence of resonances. The solid curve which uses $E_0 = -20$ eV, $\Gamma_n^0 = 129$ meV, $\Gamma_\gamma = 75$ meV and $R' = 7.9$ fm gives a best fit without considering the known partial thermal cross sections. The dashed curve which uses $E_0 = -25$ eV, $\Gamma_n^0 = 160$ meV, $\Gamma_\gamma = 65$ meV and $R' = 7.5$ fm is the best fit when the parameters are required to fit the thermal capture and scattering cross sections (Ref. 5). The latter solution is preferred.

be less than or equal to the abscissa value for a level population of the observed size, for the O.E. theory, and for the U.W. theory (uncorrelated set of adjacent Wigner distributed spacings). The value of $P_<$ is only 0.017 for the U.W. case (very unlikely), but is 0.61 for the now favored O.E. theory case. Figure 9(c) shows a comparison with Dyson's F test which is described by Liou, Camarda, and Rahn.[9] The values remain in the region -2σ to $+2\sigma$, indicating agreement with the concept of no lost s levels or spurious extra levels. Figure 9(d) shows the plot of $\sigma(k)$ vs k of the standard deviation from their mean for the spacings of levels having k levels between (in units of $\langle D\rangle$). This type of plot was suggested by Bohigas and Flores[10] when it seemed that earlier, poorer, data gave better agreement with their TBRE (two-body random Hamiltonian ensembles) than with the O.E. theory. As with ^{166}Er (VIII) and our other[9] good test cases, we find best agreement with the O.E. theory predictions.

Population corrections for ^{174}Yb and ^{176}Yb were made in a manner similar to those which we have previously used for ^{168}Er and other cases (VIII). For ^{174}Yb, the net correction involved deleting the level at 1635 eV as "probably being a p level" and adding a "missed s level" at 1485 eV. The calculations were done in two parts. First, we studied the data to establish our probable "threshold detection sensitivity value for Γ_n^0 vs E." This suggests that about one s level was missed to 3.3 keV. Similarly, for various choices of the p strength function, S_1, one can calculate[11] the relative "*a posteriori*" probability that each observed weak level be p (rather than s). The level at 1635 eV has the highest probability, p, of being a p level with $p>0.5$ for $10^4 S_1 \geq 0.5$. It was, therefore, deleted from the s population. The next logic point is "where should the missed s level be placed?" The biggest level spacing then was for the interval where the p level had been deleted. The "missed" s level was put in the center (1485 eV) of the spacing interval.

Figure 10(a) shows the Dyson-Mehta Δ test ap-

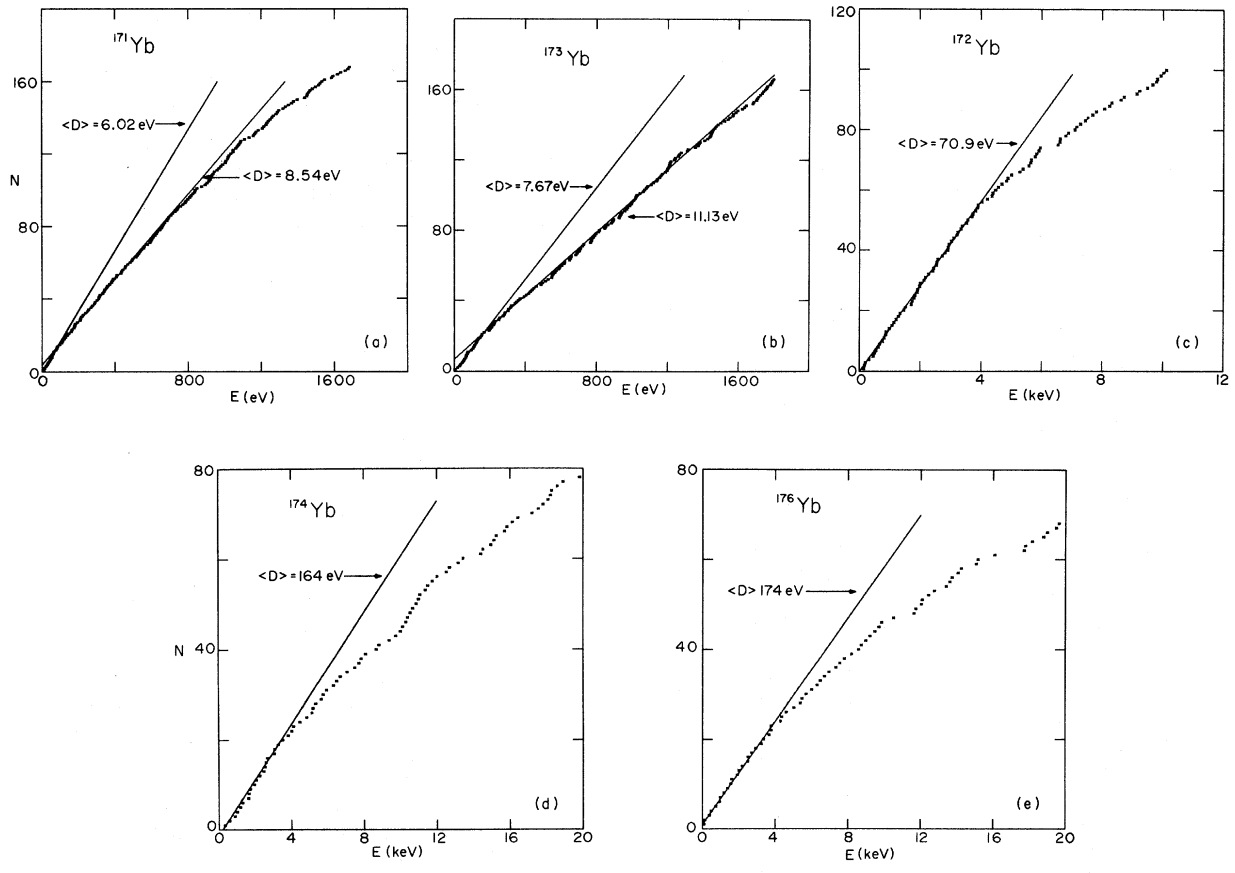

FIG. 5. Plots of the cumulative level count vs energy for (a) ^{171}Yb, (b) ^{173}Yb, (c) ^{172}Yb, (d) ^{174}Yb, (e) ^{176}Yb. The indicated $\langle D\rangle$ values represent only the slopes of visually fitted straight lines and do not consider the possibility of some missed weak s levels or included p levels. The best choice s level $\langle D\rangle$ values are given in Table IX.

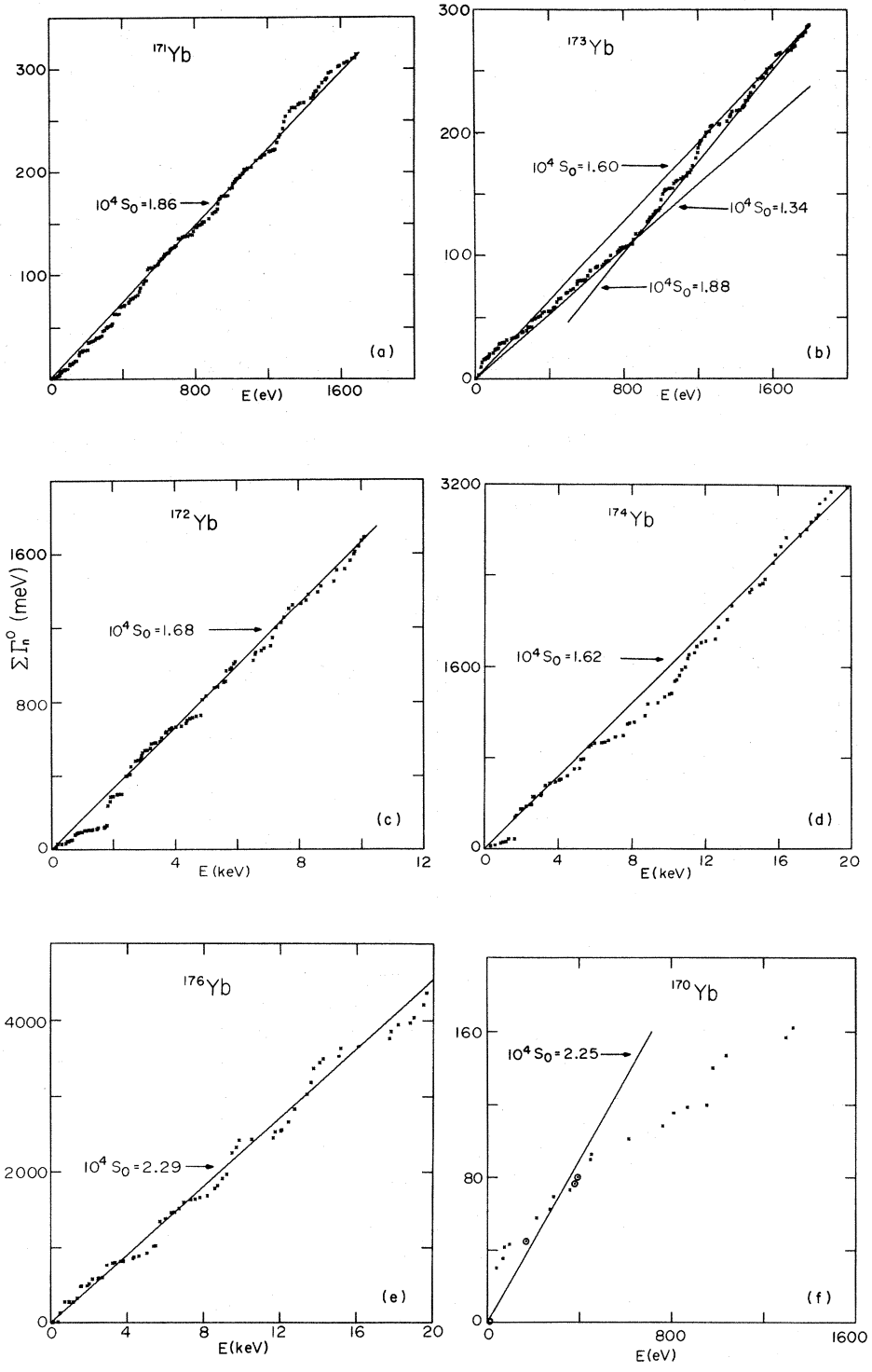

FIG. 6. Plots of $\sum g\Gamma_n^0$ or $\sum \Gamma_n^0$ vs energy for (a) ^{171}Yb, (b) ^{173}Yb, (c) ^{172}Yb, (d) ^{174}Yb, (e) ^{176}Yb, (f) ^{170}Yb. The slopes of the fitted straight lines give the s-wave strength functions. In (f) the "⊙" levels are from Ref. 5, since we miss many ^{170}Yb levels in natural Yb due to level structure of the other more abundant isotopes.

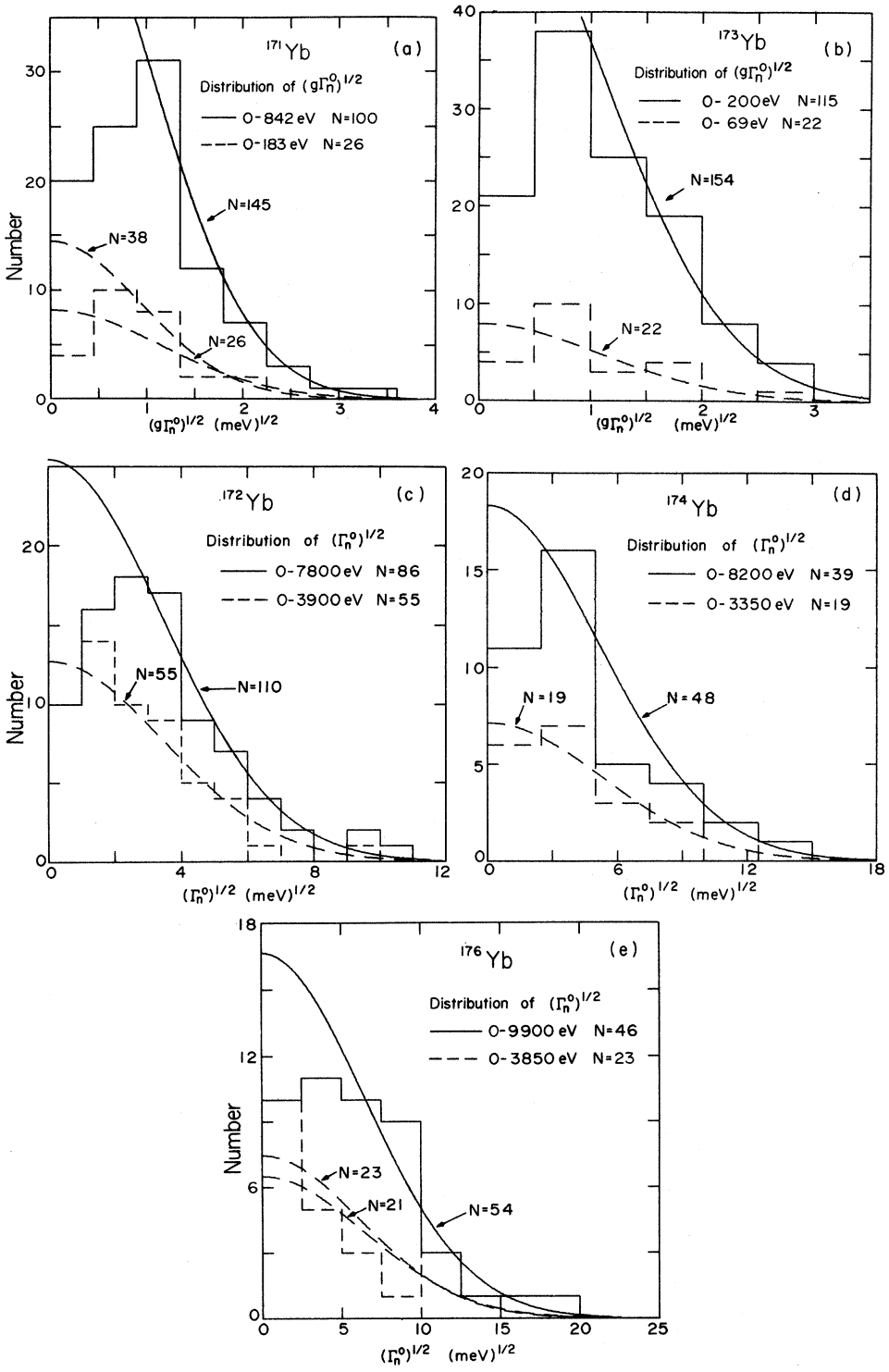

FIG. 7. Histograms of $(g\Gamma_n^0)^{1/2}$ or $(\Gamma_n^0)^{1/2}$ values for (a) ^{171}Yb, (b) ^{173}Yb, (c) ^{172}Yb, (d) ^{174}Yb, (e) ^{176}Yb. In each isotope case, histograms are shown separately for two energy intervals. They are compared with Porter-Thomas single-channel curves which are normalized to the experimental S_0 value, but with the total number of levels in each energy interval treated as a fitting parameter for the upper part of the histogram.

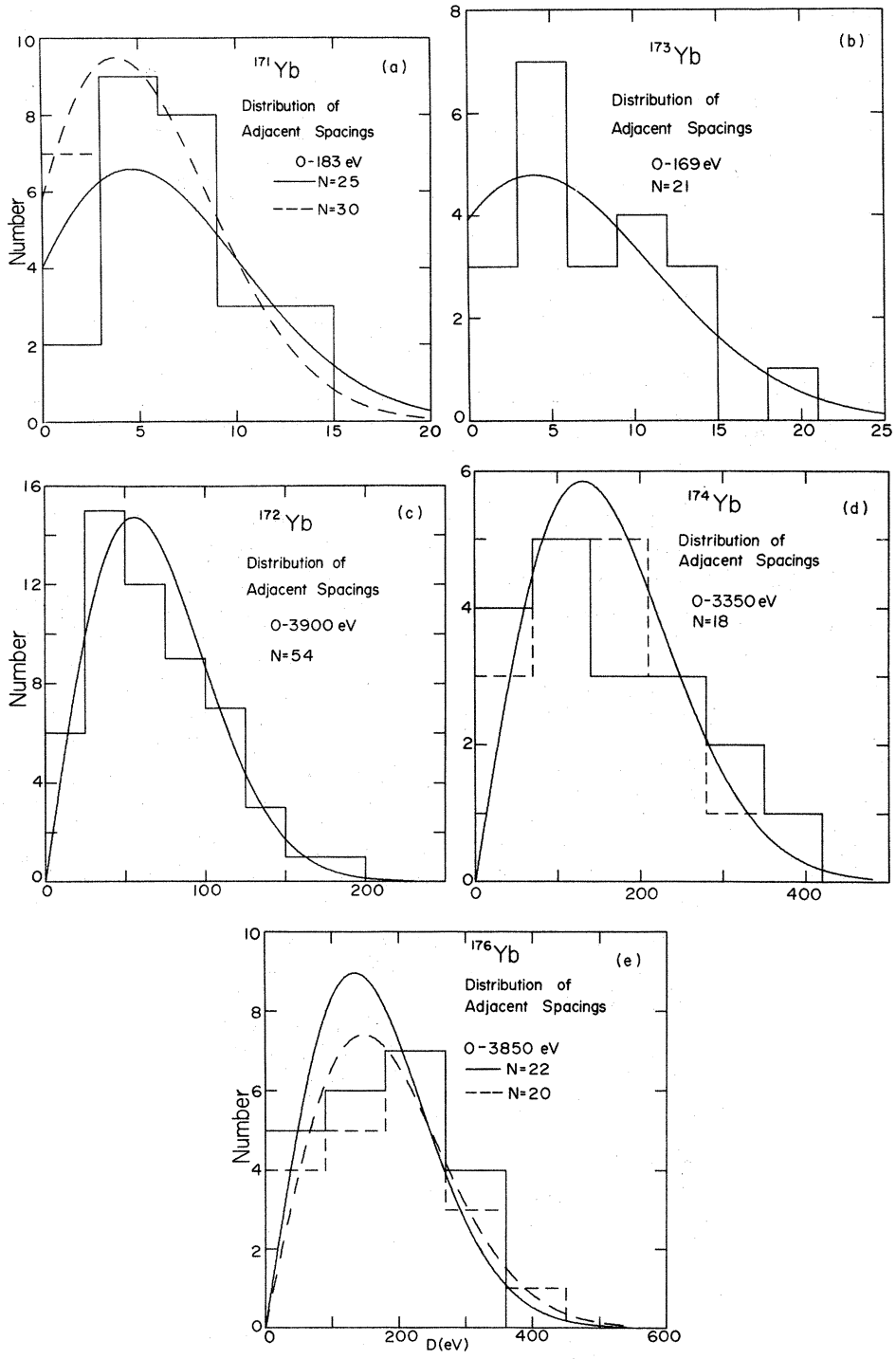

FIG. 8. Plots of the nearest level spacing distributions and the comparison Wigner curves (normalized to a fitted number of spacings) for (a) ^{171}Yb, (b) ^{173}Yb, (c) ^{172}Yb, (d) ^{174}Yb, (e) ^{176}Yb. For ^{171}Yb and ^{173}Yb, the theoretical curves are for a merged two-population distribution with the relative density as the ratio of $(2J+1)$ values. Plot (c) shows an excellent agreement between the experimental histogram and the Wigner curve. For ^{174}Yb and ^{176}Yb, the solid histograms correspond to the observed spacing distributions, while the dashed histograms correspond to the altered distributions as described in the text.

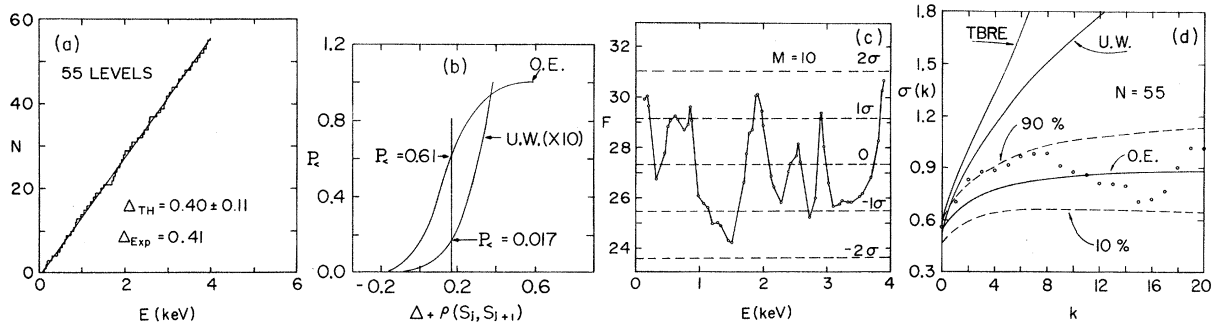

FIG. 9. (a) Best straight line fit to N vs E for 55 observed levels in ^{172}Yb to 3900 eV. This gives $\Delta_{Exp}=0.41$ vs the Dyson-Mehta predicted value of 0.40 ± 0.11. (b) A plot of the probability for a measured $\Delta+\rho$ for the 55 levels in ^{172}Yb is 0.017 for the U. W. case and 0.61 for the O.E. case. (c) Plot of successive Dyson's F statistic values for the 55 levels in ^{172}Yb. Shown are also the O.E. theory predicted average value and its 1 and 2 standard deviation limits. (d) Comparison of experimental ^{172}Yb to 3900 eV for $\sigma(k)$ vs k with Monte Carlo results for the cases of O.E., U.W., and TBRE. Here $\sigma(k)$ is the standard deviation from their mean for the spacings of levels having k levels between (in units of $\langle D\rangle$). The dashed curves give the 10 and 90% confidence limits for O.E.

plied to the "corrected" ^{174}Yb levels to 3350 eV. The predicted Δ is 0.29 ± 0.11 vs experimental Δ values of 0.31 (modified) and 0.39 before modification. The $\rho(S_j, S_{j+1})$ values are -0.35 and -0.36 for the observed and modified level sets, respectively, vs (-0.27 ± 0.22) expected from O.E. theory. Tests of $P_<$ for the $\Delta+\rho$ values gave 0.31 and 0.13 for the O.E. and U.W. cases, respectively, using the modified level set.

For ^{176}Yb, the "modified set" was obtained by deleting three weak levels as p levels and adding one "missed weak s level." The choice of one missed s level was made from calculations of the expected number of missed s levels to 3850 eV. The choice of weak levels as "p levels" was similarly made using a Bayes theorem analysis. For $10^4S_1=0.7$, we expect to see three levels. For $10^4S_1=0.8$, the Bayes theorem analysis gives $\Sigma p=3.7$ for weak levels being p levels, with $p=0.56$, 0.82, and 0.69, respectively, for levels at 950, 993, and 3361 eV and with $p\leq0.46$ for all other weak levels. This "established" the choice of the three levels deleted as p levels. The "missed weak s level" was placed at 954 eV, at the middle of the largest resulting spacing interval. This somewhat improves the poor fit of Fig. 8(e) for the spacing distribution. Figure 10(b) shows the Dyson-Mehta Δ test for the modified ^{176}Yb level set to 3850 eV. The experimental $\Delta=0.34$ is in good agreement with the predicted $\Delta=0.30\pm0.11$ of O.E. theory. Before modification, we have $\Delta=0.28$ vs 0.31 ± 0.11 predicted. The values of $\rho(S_j, S_{j+1})$ before and after modification are -0.47 and -0.20, respectively, vs an O.E. value of -0.27 ± 0.20. The sample size is too small to have $\Delta+\rho$ represent a serious test for $P_<$ to distinguish the O.E. and U.W. cases. The $P_<$ values are 0.61 and 0.23 for the modified set and 0.08 and 0.02 for the original set. It is seen that these statistical tests were more favorable to the O.E. theory before the modification. The "final choice" selections for the mean s level spacings $\langle D\rangle$ and strength functions, S_0, are summarized in Table IX.

Our partially processed Yb data, in a format of "sample cross section" vs channel energy, are on file at the BNL Center.[12] The stated energy uncertainties in this paper usually correspond to the energy separation of adjacent timing channels. The stated uncertainties in the Γ_n^0 and Γ_γ values are judgment estimates intended to include all uncertainties, including estimated systematic uncertainties, such that there is $\sim\frac{2}{3}$ probability that the true value is within the stated limits on the average. The stated uncertainties in the strength function are standard deviation values based only on the number of levels involved. The indicated uncertainties in the $\langle D\rangle$ values of Table IX are inversely proportional to the number of levels, n,

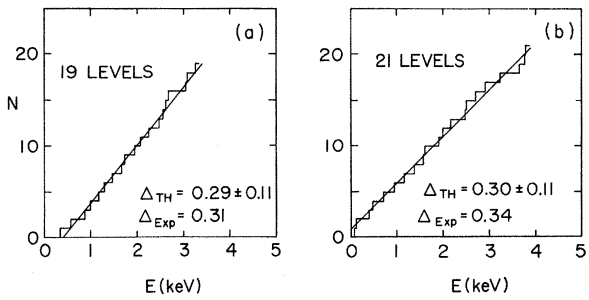

FIG. 10. Plots of the Dyson-Mehta Δ test applied to (a) the modified ^{174}Yb levels to 3350 eV, and (b) the modified ^{176}Yb levels to 3850 eV.

as required by O.E. theory. The numerator is the value implied by O.E. theory, 1 for even A or 1.5 for odd A, increased by unity to include the effect of ± 1 uncertainty in the measured n for the interval. More detailed discussion of some of these matters is given in Ref. 7.

ACKNOWLEDGMENTS

The computer interface system was developed by the Pegram Laboratory electronics group under Dr. Jack Hahn, with contributions by Dr. Hugo Ceulemans. The technical support by the late Arthur Blake, Lester Morganstein, and William Van Wart was important. Dr. George Rogosa and his colleagues at the U. S. Atomic Energy Commission provided essential help in procuring the separated isotope samples. Finally, we thank Ms. Ann Therrien for typing the manuscript.

---

†Research supported in part by the U. S. Atomic Energy Commission.

*Present address: National Bureau of Standards, Gaithersberg, Maryland.

‡Present address: University of Capetown, Republic of South Africa.

[1]Earlier papers in this series: I, J. L. Rosen, J. S. Desjardins, J. Rainwater, and W. W. Havens, Jr., Phys. Rev. 118, 687 (1960), U^{238}; II, J. S. Desjardins, J. L. Rosen, W. W. Havens, Jr., and J. Rainwater, *ibid.* 120, 2214 (1960), Ag, Au, Ta; III, J. B. Garg, J. Rainwater, J. S. Petersen, and W. W. Havens, Jr., *ibid.* 134, B985 (1964), Th^{232}, U^{238}; IV, J. B. Garg, W. W. Havens, Jr., and J. Rainwater, *ibid.* 136, B177 (1964), As, Br; V, J. B. Garg, J. Rainwater, and W. W. Havens, Jr., *ibid.* 137, B547 (1965), Nb, Ag, I, Cs; VI, S. Wynchank, J. B. Garg, W. W. Havens, Jr., and J. Rainwater, *ibid.* 166, 1234 (1968), Mo, Sb, Te, Pr; VII, J. B. Garg, J. Rainwater, and W. W. Havens, Jr., Phys. Rev. C 3, 2447 (1971), Ti, Fe, Ni; VIII, H. I. Liou *et al.*, *ibid.* 5, 974 (1972), Er; IX, F. Rahn *et al.*, *ibid.* 6, 251 (1972), Sm, Eu; X, F. Rahn *et al.*, *ibid.* 6, 1854 (1972), ^{232}Th, ^{238}U. Papers referred to by Roman numerals in the text.

[2]H. S. Camarda *et al.*, in *Statistical Properties of Nuclei*, edited by J. B. Garg (Plenum, New York, 1972), pp. 205–213.

[3]C. M. Newstead *et al.*, in *Statistical Properties of Nuclei* (see Ref. 2), pp. 367–375.

[4]*Neutron Cross Section*, compiled by M. D. Goldberg *et al.*, Brookhaven National Laboratory Report No. BNL 325 (U. S. GPO, Washington, D. C., 1966), 2nd ed., Suppl. No. 2.

[5]S. Mughabghab and R. E. Chrien, Phys. Rev. 174, 1400 (1968).

[6]H. I. Liou, Ph.D. thesis, Columbia University, 1968 (unpublished).

[7]H. I. Liou and J. Rainwater, Phys. Rev. C 6, 435 (1972).

[8]The series of papers by Professor F. Dyson alone and with Dr. Mehta are as follows: F. J. Dyson, J. Math. Phys. 3, 140, 157, 166, 1199 (1962), denoted I, II, III, and T.F.W.; and F. J. Dyson and M. L. Mehta, *ibid.* 4, 701, 713 (1963), denoted IV and V. (Δ_3 statistic is described in paper IV.)

[9]H. I. Liou, H. S. Camarda, and F. Rahn, Phys. Rev. C 5, 1002 (1972).

[10]O. Bohigas and J. Flores, in *Statistical Properties of Nuclei*, (see Ref. 2), pp. 195–203.

[11]L. M. Bollinger and G. E. Thomas, Phys. Rev. 171, 1293 (1968).

[12]Neutron Cross Section Center, Brookhaven National Laboratory, Upton, N.Y. 11973.